Analysis of the networked implementation of the primary circuit pressurizer controller at a nuclear power plant

G. Szederkényi, Z. Szabó, J. Bokor and K.M. Hangos

***Abstract*— This paper presents the $\mathcal{L}_2$ stability analysis of a networked pressure control system implemented in a nuclear power plant. The theoretical background for the applied modelling, identification, controller design tools and for the implementation process is also briefly discussed. To ensure the nominal stability properties of the designed controller in the networked environment the maximum allowable transmit interval (MATI) is computed based on the derived system model and the dynamic inversion based controller equations. This turns out to be sufficiently larger than the actual sampling interval. Simulations show good agreement with the theoretical computation results.**

I. INTRODUCTION

The continuously increasing (and sometimes conflicting) demands related to the safer, more effective and environmentally more friendly operation of complex plants often necessitates the reconstruction or even complete re-design of different subsystems. In many cases, the simplest (and cheapest) way to substantially influence important dynamical processes is the detailed modelling and model-based advanced feedback design for the affected components of the system.

One example for such a procedure is the successful modelling, identification and dynamic inversion based controller design for stabilizing the primary circuit pressure at the Paks Nuclear Power Plant in Hungary in 2004-2005 (see, e.g. [8], [10]). This controller implementation (together with other important reconstruction steps) largely contributed to the possibility that the average thermal power of the plant units could be increased by 1-2%. The implemented controller is a redundant networked control system (a redundant NCS), where the measurement results and the control commands are transferred to the computing units and actuators through an Ethernet network. The controller was originally designed in continuous time and then it was discretized using an appropriate sampling interval. However, because of the complex scheduling of network resources, possible transmission delays, faults, invalid measurements, other tasks with higher priority etc., it is hard to guarantee (even after a very careful design process) that exactly at each scheduled sampling instant a correctly computed input command is transferred to the actuators. Therefore the analysis of the dynamic properties (particularly stability) of networked control systems has become extremely important, because of the safety critical nature of this control application.

All the authors are with the Systems and Control Laboratory, Computer and Automation Research Institute of the Hungarian Academy of Sciences, PO. Box 63, H-1518 Budapest, Hungary {szeder,szaboz,bokor,hangos }@sztaki.hu

In recent years, significant and well-usable theoretical results appeared in the field of dynamic analysis of NCSs [6], [5], [9]. The aim of this paper is to apply these results to the above mentioned networked pressure control system.

II. BASIC NOTIONS

A. Dynamic inversion based control

In order to design an advanced controller for the pressurizer, the reference tracking problem of a Wiener system, i.e. an interconnection of an LTI system with a static output nonlinearity, has to be solved. In this section the design of the dynamic inverse of the linear part of the Wiener model will be presented following [8] where more details can be found. The unmeasured output z it is supposed to be computed using a static nonlinear inverse function that it is assumed to be given. In most of the cases, this static inverse function is provided by an identification process of a Wiener model as a spline approximation, or by an approximation given by a suitable set of orthonormal functions, e.g. Chebysev polynomials or wavelets. By this assumption, instead of the desired output y_d of the nonlinear system, one can also work with the corresponding desired output of the linear part of the system, i.e. z_d.

Let us recall that if the system is invertible, then V^*, i.e. the maximal (A,B)-invariant subspace contained in $kerC$, induces a decomposition of the linear system into:

$$\dot{x}_1 = A_{11}x_1 + A_{12}x_2 + B_1u \tag{1}$$

$$\dot{x}_2 = A_{21}x_1 + A_{22}x_2 \tag{2}$$

$$z = C_1x_1, \tag{3}$$

where $ImB = ImB_1$ and $x_1 \in V^{*\perp}$, see [1], [11]. Let us denote the subsystem formed by (1) and (3) by Σ_1 and the subsystem (2) by Σ_2.

By applying the feedback $u = F_1x_1 + F_2x_2 + v$, with $F = [F_1\ F_2]^T$ that renders V^* $(A + BF, B)$ invariant, one can obtain the system:

$$\dot{x}_1 = A_{11}x_1 + B_1v, \quad z = C_1x_1. \tag{4}$$

Let us denote this system by $\Sigma_{1,f}$. By choosing a solution F_2 of the equation $A_{12} + B_1F_2 = 0$ one can set $F_1 = 0$.

Denoting by c_i the rows of C_1 let us consider the subspace

$$span\{c_1, \cdots, c_1A_{11}^{\gamma_1}, \cdots, c_p, \cdots, c_pA_{11}^{\gamma_p}\} \tag{5}$$

where $c_iA_{11}^lB_1 = 0$, for $l < \gamma_i$, and γ_i are chosen such that the spanning vectors are linearly independent. It follows, that choosing the basis (5) for $V^{*\perp}$, one can define a coordinate transform $\mathcal{S}$ that maps x_1 to $\tilde{z}$, where

$$\tilde{z} = \left[z_1, \cdots, z_1^{(\gamma_1)}, \cdots, z_p, \cdots, z_p^{(\gamma_p)}\right]^T. \tag{6}$$

In this basis one has a particulary simple form of the decomposition (4). It follows, that

$$v = B_1^{-r} S^{-1}(\dot{\tilde{z}} - SA_{11}S^{-1}\tilde{z}) := \lambda(z), \quad (7)$$

$$x_1 = S^{-1}\tilde{z} := \zeta(z), \quad (8)$$

where B_1^{-r} is the right inverse of B_1.

The required input to track a desired output signal z_d is given by the dynamic system

$$\dot{\eta}_d = A_{22}\eta_d + A_{21}\zeta(z_d) \quad (9)$$

$$u_d = F_2\eta_d + \lambda(z_d), \quad (10)$$

provided that this input is applied to the original system started from the initial condition given by $x_0 = T^{-1}\begin{bmatrix} x_{10} \\ x_{20} \end{bmatrix}$, where x_{20} can be arbitrarily chosen but x_{10} should be set to $x_{10} = S^{-1}\tilde{z}_d(0)$.

In practice it seldom happens that one can impose on the system the required initial conditions, therefore, there will be an error in the whole state. To close the loop, a suitable linear dynamical system of the tracking error is added to the linearizing control input. By examining the "open–loop" equations (9) one can observe that it is possible to introduce an "outer–loop" by applying an error feedback, that modifies the equations (10) that define the control input. This idea is highlighted by the dotted line part of Figure 1.

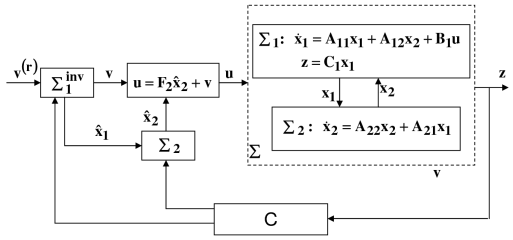

Fig. 1. Inversion based tracking

Based on this structure, an advanced (e.g. $\mathcal{H}_\infty$) controller can be designed in order to minimize the influence of the disturbances on the performance of the tracking error.

Remark 1: The dynamic inverse system for discrete systems can be obtained in a similar manner by using the shift operator $qu(t) = u(t+1)$ instead of the differentiation operator. The derivation is straightforward, hence it is omitted.

B. Analysis of networked control systems

The concepts and results summarized in this section are mostly taken from [5] and [9]. The basic configuration of a networked control system can be seen in Fig. 2, where x_p and x_c are the states of the plant and the controller, respectively, $y \in \mathbb{R}^r$ is the plant output, $u \in \mathbb{R}^p$ is the controller output, while $\hat{y} \in \mathbb{R}^r$ and $\hat{u} \in \mathbb{R}^p$ are the most recently transmitted plant and controller output values through the network. e is the error caused by network transmission that is defined as

$$e(t) = \begin{bmatrix} \hat{y}(t) - y(t) \\ \hat{u}(t) - u(t) \end{bmatrix} \quad (11)$$

Individual actuators and sensors connected to the networks are called nodes. We assume that node data are transmitted at time instants $\{t_0, t_1, \ldots, t_i\}$ where $i \in \mathbb{N}$. The transmission time instants satisfy $\epsilon < t_{j+1} - t_j \leq \tau$ for $j \geq 0$ where $\epsilon, \tau > 0$. The upper interval bound τ is called the *maximum allowable transfer interval* (MATI).

Using the notation $x = [x_p^T \quad x_c^T]^T \in \mathbb{R}^n$, the dynamic equations of a networked control system with disturbance vector $w \in \mathbb{R}^m$ between the transmission instants can be written as

$$\dot{x} = f(t, x, e, w), \quad t \in [t_{i-1}, t_i] \quad (12)$$

$$\dot{e} = g(t, x, e, w), \quad t \in [t_{i-1}, t_i] \quad (13)$$

The discontinuous change of e during transmission instants can be modeled as a jump system

$$e(t_i^+) = (I - \Psi(i, \hat{e}(t_i)))e(t_i) \quad (14)$$

$$\hat{e}(t_i^+) = \Lambda(i, \Psi(i, \hat{e}(t_i))e(t_i), \hat{e}(t_i)) \quad (15)$$

where $\hat{e}$ is the decision vector of the network scheduler, Ψ is the scheduling function and Λ is the decision update function. More details about the dynamics (14)-(15) in the case of different scheduling protocols can be found in [9]. A key feature of network scheduling protocols from the point of view of closed loop stability is the so-called *persistently exciting* (PE) property. According to the definition, a protocol is *uniformly PE in time* T if it regularly visits every network node within a fixed period of time T.

In the LTI or linearized case Eqs. (12)-(13) will be used in the form

$$\dot{x} = \Phi_{11}x + \Phi_{12}e \quad (16)$$

$$\dot{e} = \Phi_{21}x + \Phi_{22}e \quad (17)$$

where Φ_{ij} are constant matrices of appropriate dimensions. Let us introduce the following notations. $\mathcal{A}_n^+$ denotes the

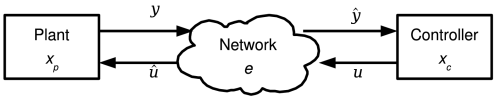

Fig. 2. Networked control system

set of positive semidefinite symmetric $n \times n$ matrices with positive entries. For $x, y \in \mathbb{R}^n$, $x \preceq y \iff x_i \leq y_i$ for $i = 1, \ldots, n$. For an n-dimensional vector x, $\bar{x} = [|x_1|, \ldots, |x_n|]^T$. The following theorem from [9] will serve as a theoretical basis for our forthcoming calculations in section IV-C.

Theorem 1: Suppose that the NCS scheduling protocol of (12)-(15) is uniformly persistently exciting in time T and the following assumptions hold

1) There exist $Q \in \mathcal{A}_n^+$ and a continuous output of the form $\tilde{y}(x, w) = G(x) + w$ so that the error dynamics (13) satisfies
$$\bar{g}(t, x, e, w) \preceq Q\bar{e} + \tilde{y}(x, w) \quad (18)$$
for all (x, e, w), for $t \in (t_i, t_{i+1})$, and for all $i \in \mathbb{N}$.
2) (12) is $\mathcal{L}_p$ stable from (e, w) to $G(x)$ with gain γ for some $p \in [1, \infty]$.
3) the MATI satisfies $\tau \in (\epsilon, \tau^*)$, $\epsilon \in (0, \tau^*)$, where
$$\tau^* = \ln(v)/(|Q|T), \quad (19)$$

and v is the solution of

$$v(|Q| + \gamma T) - \gamma T v^{1-1/T} - 2|Q| = 0. \qquad (20)$$

Then the NCS is $\mathcal{L}_p$-stable from w to $(G(x), e)$ with linear gain.

Using Theorem 1, a sharp and practically usable estimation can be obtained for the acceptable upper bound of the MATI such that the $\mathcal{L}_p$ stability of the closed loop system is preserved.

III. SYSTEM DESCRIPTION

A. Environment and operating principles of the pressurizer

The Paks Nuclear Power Plant (NPP) is situated in the south of Hungary and it operates four VVER-440/213 type reactor units with a total nominal (electrical) power of 1860 MWs (about 40 percent of the electrical energy generated in Hungary is produced there). The VVER-440 type units belong to the group of pressurized water reactors (PWRs). The most important structural components of PWRs are the *active zone*, the *primary circuit* and the *secondary circuit*. The controlled nuclear chain reaction is taking place in the active zone, where the fuel rods made of uranium dioxide and the absorbent control rods are located. The function of the primary circuit is to transfer the heat generated in the active zone towards the secondary circuit. Therefore the water in the primary circuit is circulated at high speed by powerful circulation pumps. In PWRs the water in the primary circuit is not boiling which is achieved by maintaining high pressure (approximately 123 bars) using an electrically heated pressurizer unit. The steam generator is essentially a huge heat exchanger, where a significant part of the primary circuit heat is transferred to the secondary circuit. This heat is converted to mechanical and finally to electrical energy in the secondary circuit. The water of the secondary circuit in the steam generator is boiling and the vapor going out of the steam generator rotates the turbines that produce electrical energy.

The task of the pressurizer is to keep the pressure within a predefined range. The pressurizer is a vertical tank and inside this tank there is hot water at a temperature of about 325°C and steam above. If the primary circuit pressure decreases, electric heaters switch on automatically in the pressurizer (see Fig. 3) Due to the heating more steam will evaporate and this leads to a pressure increase.

The old pressure controller used a hysteresis-based switching algorithm which was basically the following. If the increasing pressure in the pressurizer reached a certain limit, firstly the heaters were turned off and then cold water was injected into the tank (if needed) to reduce the pressure down to the predefined range [7]. The electric heater consisted of four heating elements (each with 90 kWs of power) of discrete operation (on/off) mode, that is, the system input was an integer from the set $\{0, 1, 2, 3, 4\}$ describing the number of heating elements that were turned on. Moreover, the accuracy of the pressure measurements was not very good with a measurement error of $\pm 0.15\%$.

Using this old technology, the primary circuit pressure was oscillating in an approximately 1 bar interval during normal operation. The high peaks of these oscillations prevented the possibility of operating the units at a slightly higher thermal power (because of safety limits). As a result of equipment modernization, the heating energy of the electric heaters can now be set in a continuous range of 0-360 kW and new pressure sensors were installed with a significantly lower measurement error. These changes made possible the design of a more advanced controller that can stabilize the pressure in a much narrower range.

The manipulable input variable of the model is the number of heating elements turned on (not necessarily integer number in the range 0–4) that is directly proportional to the instantaneous electrical heating power. Furthermore, there is an approximately constant water in- and outlet to and from the tank. The time-varying temperature of the inflowing water will be treated as a disturbance in the model. The controlled and measured output is the pressure in the tank (see Fig. 3).

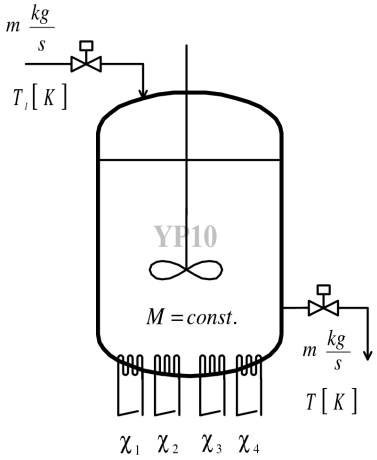

Fig. 3. Simplified structure of the pressurizer

B. System modelling

The physical modelling of the primary circuit dynamics (including the pressurizer) has been carried out following the principles of [3] and is described in greater detail in [2]. The variables and constants appearing in the model are listed in Table I. The state-space model of the pressurizer model is given by

$$\dot{x} = Ax + Bu + Ed \qquad (21)$$

where the state vector x, the input u and the external disturbance vector d are

$$x = [T\ T_W]^T,\ u \in [0, 4],\ d = [T_I\ W_l]^T$$

The actually measured pressure is a nonlinear static function of the water temperature in the following form

$$p = h(T) = \frac{e^{\varphi(T)}}{100}$$

T	water temperature	°C
T_W	tank wall temperature	°C
c_p	specific heat of water	$\frac{\text{J}}{\text{kg°C}}$
U	internal energy of water	J
U_W	internal energy of the wall	J
m	mass flow rate of inlet water	$\frac{\text{kg}}{\text{s}}$
T_I	inlet water temperature	°C
M	mass of water	kg
C_{pW}	heat capacity of the wall	$\frac{\text{J}}{\text{°C}}$
W_{HE}	power of one electric heater	W
W_l	environmental heat loss	

TABLE I

VARIABLES AND CONSTANTS OF THE PRESSURIZER MODEL

where $\varphi(T) = c_0 + c_1 T + c_2 T^2 + c_3 T^3$ with constants $c_0, \ldots, c_3$. Therefore the output equation can be written as

$$y = \begin{bmatrix} 1 & 0 \end{bmatrix} x, \quad x_1 = h^{-1}(p) \tag{22}$$

The matrices of the model are

$$A = \begin{bmatrix} -\frac{m}{M} - \frac{K_W}{c_p M} & \frac{K_W}{c_p M} \\ \frac{K_W}{C_{pW}} & -\frac{K_W}{C_{pW}} \end{bmatrix} \tag{23}$$

$$B = \begin{bmatrix} \frac{W_{HE}}{c_p M} \\ 0 \end{bmatrix}, \quad E = \begin{bmatrix} \frac{m}{M} & 0 \\ 0 & \frac{1}{C_{pW}} \end{bmatrix}$$

Considering the already mentioned nonlinear dependence of pressure on temperature, the model falls into the class of Wiener systems that can be described with a linear dynamics plus an output nonlinearity. To validate the proposed model structure, the theory of elementary subsystem (ESS) representation [4] was used successfully. Although acceptable values for $c_0, \ldots, c_3$ were known from physical data tables, these parameters needed to be estimated more precisely because of the boron content of the primary circuit water. Therefore the unknown parameters were separated into two vectors: $\theta_1 = [C_{pW}\ K_W\ W_l]^T$ and $\theta_2 = [c_0\ c_1\ c_2\ c_3]^T$. Then, an iterative procedure based on prediction error minimization was constructed for the estimation of θ_1 and θ_2, which converged well. The detailed identification procedure is described in [10].

IV. CONTROL SYSTEM ANALYSIS

The main control goal is to stabilize the pressure at a prescribed reference value (typically around 123-124 bars which is equivalent to approximately 327 °C in terms of temperature). Moreover, the controller's additional task is to suppress the effect of measurement noise and that of the time-varying disturbances (W_l, T_I).

A. Controller description

Using the theory described in section II-A, the brief summary of the controller design method is the following. The state-space equations of the open loop system (21) can be rewritten as

$$\dot{x}_1 = a_{11} x_1 + a_{12} x_2 + B_u u + E_T T_I \tag{24}$$

$$\dot{x}_2 = a_{21} x_1 + a_{22} x_2 - E_W W_l \tag{25}$$

where $a_{ij} = A_{ij}$, $B_u = B_1$, $E_T = E_{11}$ and $E_W = E_{22}$ in (23). Let x_1^r denote the reference value for x_1 (i.e. $z_d = x_1^r$). Furthermore, let us denote the nominal (mean) values for the time-varying disturbances by $T_{I,n}$ and $W_{l,n}$, respectively.

Note that the system equations (24)-(25) are already in the form of eqs. (1)-(2) with extra disturbance terms. Since $A_{11} = a_{11}$ is a scalar, we don't need the general coordinates transformation $\mathcal{S}$ described in section II-A, and the equations of the inversion controller can be derived in the following straightforward way. The dynamic equation of the inversion controller is given by

$$\dot{\eta} = a_{22}\eta + a_{21} x_1^r - E_W W_{l,n} \tag{26}$$

The input u is expressed as $u = u^r + v$, where

$$u^r = \frac{1}{B_u}(\dot{x}_1^r - a_{11} x_1^r - a_{12}\eta - E_T T_{I,n}), \tag{27}$$

and v is a new input term for additional feedback.

The state variables of the tracking error system are defined as

$$s_1 = x_1 - x_1^r, \quad s_2 = x_2 - \eta \tag{28}$$

Substituting (27) into (24) gives

$$\dot{x}_1 = a_{11}(x_1 - x_1^r) + a_{12}(x_2 - \eta) + E_T \tilde{d}_1 \tag{29}$$

where $\tilde{d}_1 = T_I - T_{I,n}$. For the tracking error dynamics, we get

$$\dot{s}_1 = a_{11} s_1 + a_{12} s_2 + E_T \tilde{d}_1 + B_u v \tag{30}$$

$$\dot{s}_2 = a_{21} s_1 + a_{22} s_2 - E_W \tilde{d}_2 \tag{31}$$

where $\tilde{d}_2 = W_l - W_{l,n}$.

Taking into consideration that x_1 is the measured state variable, we can shape the error dynamics with a dynamic (or static) controller of the general form

$$\dot{\xi} = M_{c1}\xi + M_{c2} s_1 \tag{32}$$

$$v = M_{c3}\xi + M_{c4} s_1, \tag{33}$$

for details, see [8].

B. Controller implementation

The hardware environment of the controller implementation is a distributed digital system. The functional units of the system are connected through an Ethernet network. The pressure is measured by a high precision instrument located in a hermetically sealed area. The data are transferred to a Siemens S300 control unit using the Profibus PA protocol. The pressure measurement loop has a redundant architecture. The S300 controller checks the status of the pressure measurements and transfers them to other nodes of the network. It can also check signal values during tests. The endpoints of the system are Wago intelligent controllers that actually operate the electric heaters and valves. These devices, located at different points of the power plant, are the real physical actuators in the system. The three controllers work cooperatively: their states are shared with each other and with the central computer system. They are also able to work in reduced mode independently in case of certain failures. The structural diagram of the implemented system is shown in Fig. 4.

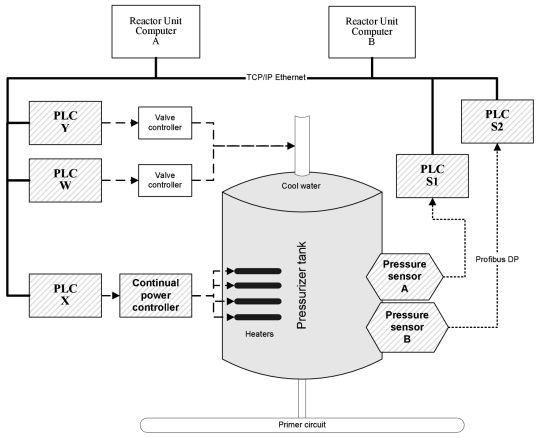

Fig. 4. Architecture of the redundant control system

C. Dynamic analysis of the networked control solution

For the simplification of the forthcoming calculations, we will use the following (sometimes simplifying) assumptions for the analysis.

- $\mathcal{A}1$ The time-varying disturbances T_I and W_l are constant. This assumption approximates reality quite well if we consider a few minutes to approximately one hour of system operation, because the change of these disturbances is usually rather slow compared to the system dynamics.
- $\mathcal{A}2$ The nominal values of disturbances ($T_{I,n}$, $W_{l,n}$) are constant.
- $\mathcal{A}3$ Zero order hold is assumed on the input.
- $\mathcal{A}4$ The temperature reference x_1^r is (at least piecewise) constant.
- $\mathcal{A}5$ Pressure measurement noise is not taken into consideration during the analysis.
- $\mathcal{A}6$ Similarly to the examples in [9], all the network induced errors are grouped to the output, i.e. $e = \hat{y}(t) - y(t)$.

The analyzed dynamic inversion based controller uses a static error feedback, therefore the controller equations (26), (27) and (33) can be summarized in the following simple state-space model containing only one state variable (denoted by x_3):

$$\begin{aligned} \dot{x}_3 &= A_c x_3 + B_{c1} x_1 + (B_{c1} - B_{c4}) x_1^r + B_{c3} W_{l,n} \\ y_c &= D_{c4} x_1 + C_c x_3 + (D_{c1} - D_{c4}) x_1^r + D_{c2} T_{I,n} \end{aligned}$$

where A_c, B_{ci}, C_c and D_{ci} are the controller parameters, and x_1 is the temperature in the pressurizer. The actual system input can be computed as

$$u = y_c + e \tag{34}$$

Using (34), the equations of the closed loop system can be written as

$$\begin{aligned} \dot{x}_1 &= (a_{11} + B_u D_{c4}) x_1 + a_{12} x_2 + B_u C_c x_3 + E_T T_I \\ &\quad + B_u (D_{c1} - D_{c4}) x_1^r + B_u D_{c2} T_{I,n} + B_u e \qquad (35) \\ \dot{x}_2 &= a_{21} x_1 + a_{22} x_2 + E_W W_l \qquad (36) \\ \dot{x}_3 &= B_{c4} x_1 + A_c x_3 + (B_{c1} - B_{c4}) x_1^r + B_{c3} T_{I,n} \qquad (37) \\ y_c &= D_{c4} x_1 + C_c x_3 + (D_{c1} - D_{c4}) x_1^r + D_{c2} T_{I,n} \qquad (38) \end{aligned}$$

Observe, that we have a LTI closed loop system model. Therefore, from Eqs. (35)-(37), matrices Φ_{11} and Φ_{12} in (16) are obtained as

$$\Phi_{11} = \begin{bmatrix} a_{11} + B_u D_{c4} & a_{12} & B_u C_c \\ a_{21} & a_{22} & 0 \\ B_{c4} & 0 & A_c \end{bmatrix}, \tag{39}$$

$$\Phi_{12} = \begin{bmatrix} B_u \\ 0 \\ 0 \end{bmatrix} \tag{40}$$

Let us denote the ith row of Φ_{11} by Φ_{11}^i. Using assumptions $\mathcal{A}1$–$\mathcal{A}4$, the time derivative of e can be written as

$$\begin{aligned} &\dot{e} = -\dot{y}_c = -D_{c4}\dot{x}_1 - C_c \dot{x}_3 = \\ &-D_{c4}\Phi_{11}^1 x - C_c \Phi_{11}^3 x - D_{c4} B_u e - D_{c4} E_T T_I - \\ &D_{c4} B_u (D_{c1} - D_{c4}) x_1^r - D_{c4} B_u D_{c2} T_{I,n} - \\ &C_c (B_{c1} - B_{c4}) x_1^r - C_c B_{c3} W_{l,n} \end{aligned} \tag{41}$$

From (41), matrices Φ_{21} and Φ_{22} of (17) are the following

$$\Phi_{21} = -D_{c4}\Phi_{11}^1 - C_c \Phi_{11}^3 \tag{42}$$

$$\Phi_{22} = -D_{c4} B_u \tag{43}$$

The matrices of the continuous time system model were the following:

$$\begin{aligned} A &= \begin{bmatrix} -2.7099 & 2.7011 \\ 2.9864 & -2.9864 \end{bmatrix} \cdot 10^{-3}, \\ B &= \begin{bmatrix} 1.2653 \cdot 10^{-3} \\ 0 \end{bmatrix}, \quad E_T = 8.8 \cdot 10^{-6}, \\ E_W &= -1.55 \cdot 10^{-8} \end{aligned} \tag{44}$$

The controller parameters were

$$\begin{aligned} &A_c = -0.0029,\ B_{c1} = 0.0029,\ B_{c3} = -0.0020, \\ &B_{c4} = 0.011,\ C_c = -2.1031,\ D_{c1} = 2.11, \\ &B_{c2} = -0.007,\ B_{c4} = -7.58 \end{aligned} \tag{45}$$

From the above, the following numerical values were obtained for the matrices in (16)-(17)

$$\begin{aligned} \Phi_{11} &= \begin{bmatrix} -0.0123001 & 0.0027011 & -0.0026610 \\ 0.0029864 & -0.0029864 & 0. \\ 0.0110168 & 0. & -0.0029460 \end{bmatrix}, \\ \Phi_{12} &= \begin{bmatrix} 0.0012653 & 0 & 0 \end{bmatrix}^T, \\ \Phi_{21} &= \begin{bmatrix} -0.0700599 & 0.0204731 & -0.0263650 \end{bmatrix}, \\ \Phi_{22} &= 0.0095902 \end{aligned} \tag{46}$$

Since the system is SISO, the number of network links can chosen to be one, i.e. $T = 1$.

The $\mathcal{L}_2$ gain between the error e and the output $\tilde{y} = \Phi_{21} x$ is $\gamma = 9.595 \cdot 10^{-3}$. For the estimation of τ^*, first we solve Eq. (20) that yields $z = 1.499$. The norm of Φ_{22} is easy to compute and thus: $|\Phi_{22}| = |Q| = 9.5902 \cdot 10^{-3}$.

From these results and by solving (20), we obtain the following estimate for the MATI: $\tau^* = 42.27$ s. This proves, that the present sampling time of 10 s is a safe value from the point of view of $\mathcal{L}_2$ stability even if there are some network induced delays that do not violate τ^*.

D. Simulation results

To check the obtained results, 24 hours of system operation have been examined on simulations in Matlab/Simulink. The time function of the disturbance T_I is shown in Fig. 5, while W_{loss} was constant. The reference value for the pressure was 124 bars. White measurement noise was assumed on the output with power spectral density of 0.01. The noisy pressure measurements were converted to temperature using the same spline functions as in the real implementation. The sampling time of the controller was 10 s with zero order hold on the input. The effect of various network delays have been investigated. Fig. 6 shows the pressure values in the case of no network delay, 40s delay and 100s delay, respectively. The simulation results seem to support the former calculations. The control performance is slightly worse (but still acceptable) in the case of 40s delay, and the performance degradation is more apparent when the delay is 100s.

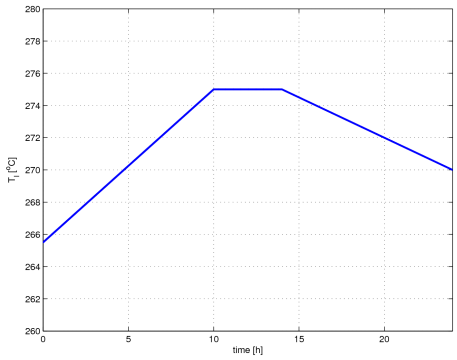

Fig. 5. Time function of disturbance T_I

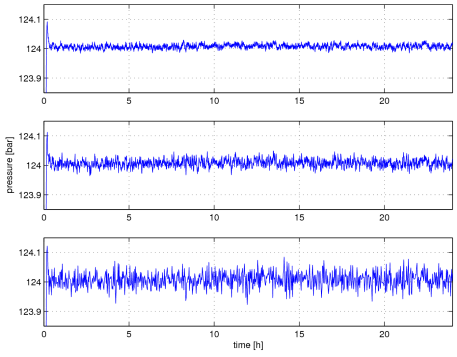

Fig. 6. Pressure in the controlled system with a) no network delay, b) 40s network delay, c) 100s network delay

V. CONCLUSIONS

The networked control solution of a pressure controller at a nuclear power plant was described and analyzed in this paper. Using the theory of networked control systems, the MATI has been computed which guarantees the $\mathcal{L}_2$ stability properties of the closed loop system. The computed MATI value has been found much larger than the sampling time of the actually implemented networked controller.

The calculations were checked against simulation results. Further work will be focused on the relaxation of some simplifying assumptions in order to obtain more accurate results for different disturbance situations.

VI. ACKNOWLEDGMENTS

The effort was sponsored by the Air Force Office of Scientific Research, Air Force Material Command, USAF, under the grant number FA8655-08-1-3016. The U.S Government is authorized to reproduce and distribute reprints for Governmental purpose notwithstanding any copyright notation thereon. This research work has been partially supported by the Hungarian Scientific Research Fund through grants no. K67625 and by the Control Engineering Research Group of the Budapest University of Technology and Economics. The first and second authors are grantees of the Bolyai János Research Scholarship of the Hungarian Academy of Sciences. The authors gratefully acknowledge the continuous support of the members of the INC Refurbishment Project at the Paks Nuclear Power Plant. The authors also thank István Varga at the Systems and Control Laboratory for his project management work.

REFERENCES

[1] G. Basile and G. Marro. A new characterization of some structural properties of linear systems: unknown-input observability, invertability and functional controllability. *Int. J. Control*, 17:931–943, 1973.

[2] Cs. Fazekas, G. Szederkényi, and K.M. Hangos. A simple dynamic model of the primary circuit in VVER plants for controller design purposes. *Nuclear Engineering and Design*, 237:1071–1087, 2007. accepted.

[3] K. M. Hangos and I. T. Cameron. *Process Modelling and Model Analysis*. Academic Press, New York, London, 2001.

[4] L. Keviczky, J. Bokor, and Cs. Bányász. A new identification method with special parametrization for model structure determination. In *5th IFAC Symposium on Identification and System Parameter Estimation, Darmstadt*, pages 561–568, 1979.

[5] D. Nesic and A.R. Teel. Input-output stability properties of networked control systems. *IEEE Transactions on Automatic Control*, 49:1650–1667, 2004.

[6] D. Nesic and A.R. Teel. Input-to-state stability of networked control system. *Automatica*, 40:2121–2128, 2004.

[7] Paks Nuclear Power Plant. VVER - 440/213 - the primary circuit, 2005. http://www.npp.hu /mukodes /tipusok /primer-e.htm.

[8] Z. Szabó, P. Gáspár, and J. Bokor. Reference tracking of Wiener systems using dynamic inversion. In *Prep. 2005 International Symposium on Intelligent Control*, pages on CD, paper ID: WeA06.5, Limassol, Cyprus, 2005.

[9] M. Tabbara, D. Nesic, and A.R. Teel. Stability of wireless and wireline networked control systems. *IEEE Transactions on Automatic Control*, 52:1615–1630, 2007.

[10] I. Varga, G. Szederkényi, K.M. Hangos, and J. Bokor. Modeling and model identification of a pressurizer at the Paks nuclear power plant. In *14th IFAC Symposium on System Identification – SYSID 2006*, pages 678–683, Newcastle, Australia, March 2006.

[11] W. M. Wonham. *Linear Multivariable Control – A Geometric Approach*. 1985.